Int. J. Solids Structures Vol. 27, No. 4, pp. 467–483, 1991
Printed in Great Britain.

0020-7683/91 $3.00 + .00

ANALYSIS OF CRITICAL BEHAVIOR OF SEMI-RIGID FRAMES WITH OR WITHOUT LOAD HISTORY IN CONNECTIONS

YOSHIAKI GOTO and SATSUKI SUZUKI
Department of Civil Engineering, Nagoya Institute of Technology, Showa-Ku, Nagoya 466, Japan

and

WAI-FAH CHEN
Structural Engineering Department, School of Civil Engineering, Purdue University, West Lafayette, IN 47907, U.S.A.

(*Received* 2 *April* 1989; *in revised form* 2 *February* 1990)

Abstract—Due to the inelastic behavior of beam-to-column connections, the critical behavior of semi-rigid frames is affected not only by the loading and unloading characteristics of connections at the critical points, but also by their load history up to these points. Thus, the stability analysis of frames of this type becomes very complicated, compared with pinned or rigid frames. Herein, we shall present a refined method which can accurately analyze the inelastic, critical behavior of semi-rigid frames, i.e. bifurcation and limit load instability. This method can also take into account the load history caused by cyclic loading. Using the proposed method, the rectangular semi-rigid frames with or without the load history due to cyclic wind load are precisely analyzed to examine their inelastic critical behavior.

1. INTRODUCTION

It is generally assumed in a conventional analysis of steel frameworks, that the beam-to-column connections are either fully rigid or ideally flexible. Although these assumptions are simple and convenient for practical design use, these highly idealized models could lose their accuracy when applied to some connections whose rigidities lie somewhere between these two extremes. In fact, most of the so-called pinned connections possess some rigidity, while the connections regarded as rigid often show some flexibility.

In view of the above, a considerable amount of study, as summarized by Jones *et al.* (1983), has been performed on the analysis of semi-rigid frames: Romstad and Subramanian (1970), Ackroyd (1979), Cook (1983), Simitses and Vlahinos (1984), Yu and Shanmugam (1986), Lui and Chen (1986), Goto and Chen (1987b), Poggi and Zandonini (1987) and Mazzolani (1987), among others. Since the moment–rotation relationships of connections mostly exhibit nonlinear behavior even at a low moment level, these studies usually consider the material nonlinearity in connections. In addition to the nonlinearity of connections, the geometrical nonlinearity has to be considered in order to analyze the stability of the frames.

The stability of a structural system is lost due to the existence of singular points on the equilibrium path, referred to as *critical points*, i.e. *bifurcation points* and *limit points*. Thus, to assess the stability, the behavior of semi-rigid frames has to be accurately analyzed around these critical points. However, owing to the inelasticity of the connections, the critical behavior of these frames is affected not only by the loading and unloading characteristics of connections at the critical points, but also by their load history up to these critical points. Thus, the stability analysis of frames of this type becomes more complicated compared with that of pinned or rigid frames.

The customary methods of analysis mostly use the simple load-control incremental method, with or without the Newton–Raphson iterative procedures and no special attention is paid to the analysis around the critical points. Consequently, customary methods cannot even give accurate information about the limit-load instability, to say nothing about the inelastic bifurcation. Furthermore, some buckling analyses determine the bifurcation load by using the secant stiffness, not the tangent stiffness of structural systems, thus yielding inaccurate results.

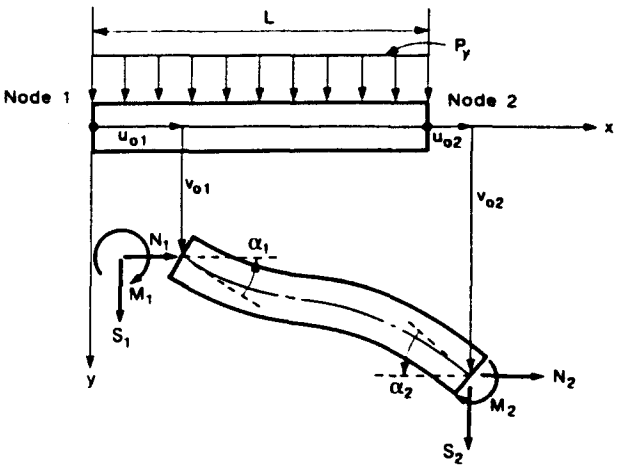

Fig. 1. Coordinate system and physical quantities for a member.

Herein, we shall present a refined method which can analyze the inelastic critical behavior of semi-rigid frames, with or without load history in connections. In the analysis of nonlinear equilibrium paths, except bifurcation points, we shall employ here the *incremental arc-length method*, combined with the *Newton–Raphson iterative procedure*. As already confirmed by Riks (1979) in elastic systems, this method can also remove the singularity at the limit point in the analysis of semirigid frames. At bifurcation points for perfect systems, solutions however, have an inherent singularity and this singularity of tangent stiffness cannot be eliminated even by the use of the arc-length method. Thus, we have developed an accurate method which can not only identify the bifurcation point, but also trace the bifurcation path. This method is rather simple because it only utilizes the tangent stiffness equations along with Hill's theory of uniqueness of elastic-plastic solids (Hill, 1958). The present analysis further implements a highly accurate connection model, based mainly on the constitutive relations obtained from experiments. The connection model includes the inelastic, cyclic behavior of semi-rigid beam-to-column connections.

Although the present analysis considers the exact geometrical nonlinearity of structural systems together with the material nonlinearity of connections, the nonlinearity due to member plastification is ignored for ease of mathematical manipulation.

Using the present method, semi-rigid frames, with or without the load history in connections, are analyzed as numerical examples to investigate the inelastic, critical behavior under vertical loads. As for the load history, the cylic wind load is considered here because of its practical importance.

2. STIFFNESS AND TANGENT STIFFNESS FOR BEAM-COLUMN MEMBER

In the derivation of the member stiffness equation, we adopt the governing differential equations of nonlinear beam-columns (Goto and Chen, 1987a), where the moderate rotations as well as the bowing of a member are considered. Using the physical quantities defined in Fig. 1, the governing equations of nonlinear beam-columns are given by the following.

Equilibrium equations

$$N' = 0, \quad (Nv_0' + M')' + p_y = 0 \tag{1a,b}$$

Boundary conditions

$$u_0 = u_{0\beta} \quad \text{or} \quad N = n_x N_\beta,$$

$$v_0 = v_{0\beta} \quad \text{or} \quad Nv_0' + M' = n_x S_\beta,$$

$$v_0' = \alpha_\beta \quad \text{or} \quad M = -n_x M_\beta, \tag{2a-c}$$

where $(\,)'$ denotes the differentiation with respect to x and n_x takes the values of -1 and $+1$, respectively, at nodes 1 and 2.

Constitutive equations

$$N = EA\{u_0' + \tfrac{1}{2}(v_0')^2\}, \quad M = -EIv_0'' \tag{3a,b}$$

In order to obtain the closed-form solution, only the y-component of a distributed force, p_y, with constant magnitude is considered in eqns (1a) and (1b) as the most important component of a distributed force. The solution so obtained is applicable to most rectangular frames. Using the summation convention, the closed-form stiffness equation for beam-columns is given in the form

$$\tilde{f}_i = \tilde{K}_{ij}(\tilde{N}_1)\tilde{d}_j + \tilde{K}_{ijk}(\tilde{N}_1)\tilde{d}_j\tilde{d}_k + \tilde{p}_y\tilde{L}_{ij}(\tilde{N}_1)\tilde{d}_j + \tilde{p}_y\tilde{L}_i(\tilde{N}_1) + \tilde{p}_y^2\tilde{C}_i(\tilde{N}_1) \tag{4}$$

where

$$^t\{\tilde{f}_i\} = (\tilde{N}_1, \tilde{S}_1, \tilde{M}_1, \tilde{N}_2, \tilde{S}_2, \tilde{M}_2), \quad ^t\{\tilde{d}_i\} = (\tilde{u}_1, \tilde{v}_1, \alpha_1, \tilde{u}_2, \tilde{v}_2, \alpha_2), \tag{5a,b}$$

$$\tilde{N}_\beta = N_\beta L^2/EI, \quad \tilde{S}_\beta = S_\beta L^2/EI, \quad \tilde{M}_\beta = M_\beta L/EI, \quad \tilde{p}_y = p_y L^3/EI,$$
$$\tilde{u}_\beta = u_{0\beta}/L, \quad \tilde{v}_\beta = v_{0\beta}/L. \tag{6a-f}$$

All the coefficients of the stiffness equation are functions of axial force N_1. Specifically, $\tilde{K}_{ij}$ and $\tilde{K}_{ijk}$ are symmetric with respect to subscripts (i, j) and (j, k), respectively. The above stiffness equation is essentially the same as that derived previously by the authors (Goto and Chen, 1987a). The only difference is that all the nodal force components, except the axial force, are eliminated on the right side of eqn (4) for ease of using the Newton-Raphson iterative procedures.

The closed-form solutions of beam-columns can be expressed by either trigonometric functions or hyperbolic functions according to whether the axial force is compressive or tensile. Furthermore, when the axial force is zero, the above solutions become indefinite and another solution, expressed by fourth-order polynomials, has to be used for this special case. Thus, usually three kinds of stiffness equations have to be used, depending on the value of the axial force. Such a procedure is cumbersome and the power-series expression (Goto and Chen, 1987a,b) is therefore introduced here, considering that both trigonometric functions and hyperbolic functions are reduced to the same expression:

$$\left.\begin{matrix}\sin \gamma L \\ \sinh \gamma L\end{matrix}\right\} = \gamma L + \gamma L \sum_{n=1}^{\infty} \frac{1}{(2n+1)!}(-\tilde{N}_1)^n, \quad \left.\begin{matrix}\cos \gamma L \\ \cosh \gamma L\end{matrix}\right\} = 1 + \sum_{n=1}^{\infty} \frac{1}{(2n)!}(-\tilde{N}_1)^n$$
$$\gamma = \sqrt{(|\tilde{N}_1|)/EI}. \tag{7a-c}$$

The adoption of the above series expansions reduces eqn (4) to exactly the same expression, regardless of whether the axial force is tensile or compressive. Moreover, it is free from numerical instability when the axial force approaches zero.

In order to carry out the Newton-Raphson iterative procedure as well as to analyze the critical points, the tangent stiffness equation is derived as follows from eqn (4), by taking the increments of $\tilde{f}_i$, $\tilde{d}_i$ and $\tilde{p}_y$:

$$\Delta\tilde{f}_i = \Delta\tilde{K}_{ij}\Delta\tilde{d}_j + \Delta\tilde{C}_i\Delta\tilde{p}_y, \tag{8}$$

where $\Delta\tilde{f}_i$, $\Delta\tilde{d}_j$ and $\Delta\tilde{p}_y$ are the increments of $\tilde{f}_i$, $\tilde{d}_j$ and $\tilde{p}_y$, respectively, and $\Delta\tilde{K}_{ij}$ and $\Delta\tilde{C}_i$ are given by

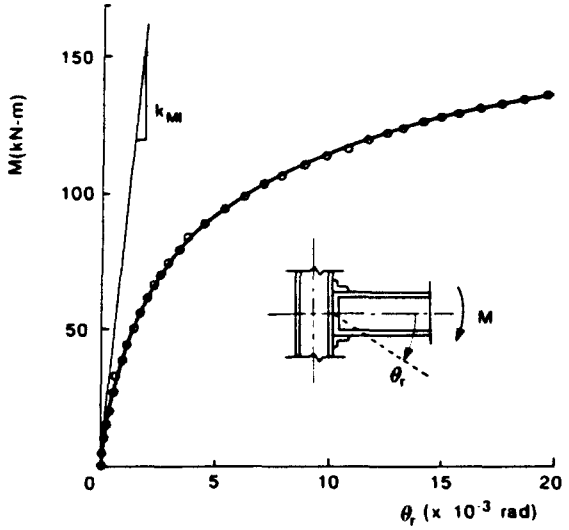

Fig. 2. Modeling of connection: ○: experimental value for top- and seat-angle connection (Hechtmann and Johnson, 1947); —: modified exponential model; k_M: initial stiffness.

$$\Delta\bar{K}_{ij} = \bar{K}_{ij} + 2\bar{K}_{ijk}\bar{d}_k + \tilde{p}_v\bar{L}_{ij} + \bar{K}_i(\bar{K}_{1j} + 2\bar{K}_{1jk}\bar{d}_k + \tilde{p}_v\bar{L}_{1j})/(1-\bar{K}_1),$$
$$\Delta\bar{C}_i = \bar{L}_{ij}\bar{d}_j + 2\tilde{p}_v\bar{C}_i + \bar{K}_i(\bar{L}_{1j}\bar{d}_j + 2\tilde{p}_v\bar{C}_1)/(1-\bar{K}_1), \tag{9a,b}$$

$$\tilde{K}_i = \frac{d\bar{K}_{ik}}{d\tilde{N}_1}\bar{d}_k + \frac{d\bar{K}_{ikm}}{d\tilde{N}_1}\bar{d}_k\bar{d}_m + \tilde{p}_v\frac{d\bar{L}_{ik}}{d\tilde{N}_1}\bar{d}_k + \tilde{p}_v\frac{d\bar{L}_i}{d\tilde{N}_1} + \tilde{p}_v^2\frac{d\bar{C}_i}{d\tilde{N}_1}. \tag{10}$$

The coefficients of the tangent stiffness equation are also expressed by the power series with respect to the axial force, for exactly the same reason as that explained in the derivation of the stiffness equation. The details of this closed-form tangent stiffness are given elsewhere (Goto *et al.*, 1991).

3. MODELING OF CONNECTIONS UNDER CYCLIC LOADING

In this study, the semi-rigid connection is represented by a discrete, inelastic, rotational spring. To express the nonlinear constitutive relations under monotonic loading for the virgin connections, the present analysis utilizes the modified exponential model (Chen and Lui, 1985; Chen and Kishi, 1989) which curve-fits the experimental data by a function of the form

$$M = k_M(\theta_r) = \sum_{i=1}^{m} A_i\{1-\exp(-\theta_r/(2ic)\} + \sum_{j=1}^{n} R_j H(\theta_r - T_j)(\theta_r - T_j), \tag{11}$$

where M is a connection moment and k_M is a function of the relative rotation, θ_r, of the connection. A_i and R_j are constants determined by the least squares method using experimental data. $H(x)$ is Heaviside's step function with respect to x, and c is a scaling factor for the exponential function.

As shown in Fig. 2, the above model represents the nonlinear connection behavior fairly well. Furthermore, this model is implemented in a data base program (Chen and Kishi, 1989) and the constitutive relations based on this model are available for various types of connections.

As for the connection behavior under cyclic loading, only few experimental data are known. Thus, it is difficult to use the curve-fitting technique to represent the constitutive relation. In our previous paper (Goto *et al.*, 1989a, 1991), the independent hardening model

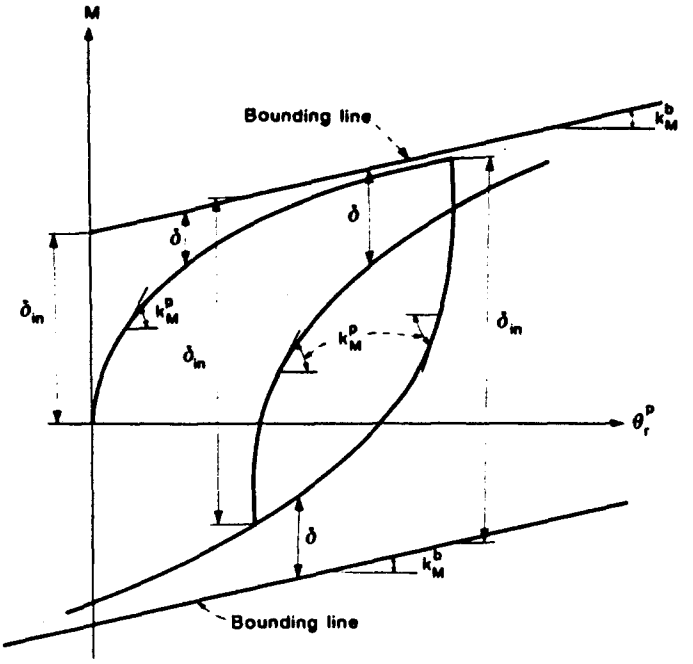

Fig. 3. Schematic illustration of bounding surface model.

is adopted for simplicity to represent the inelastic behavior. Although this model can take care of the constitutive relation under one cycle of loading, unloading and reversed loading, the connection behavior under the repetition of the above loading cycle cannot be expressed with acceptable accuracy. Thus, to overcome the deficiency of the independent hardening model, we introduce here the bounding surface model presented by Dafalias and Popov (1976) after the first unloading occurs. In this model, the plastic tangent stiffness k_M^p of the connections is approximated by

$$k_M^p = k_M^b + h\delta/(\delta_{in} - \delta), \tag{12}$$

where h is the hardening shape parameter; k_M^b is the slope of the bounding line and is determined from the experiment under monotonic loading; δ is the distance of the current moment state from the corresponding bound; and δ_{in} is the value of δ at the initiation for each loading process. These quantities are schematically shown in Fig. 3, using the moment–plastic rotation curve. From Fig. 3, the following relation holds

$$\delta = \delta_{in} + k_M^b \theta_r^p - M. \tag{13}$$

The plastic part θ_r^p of the relative rotation θ_r can be expressed as below, utilizing the initial stiffness k_{MI} of the connections:

$$\theta_r^p = \theta_r - \frac{M}{k_{MI}}. \tag{14}$$

Note that the plastic tangent stiffness of moment–rotation curves can be expressed by

$$\frac{dM}{d\theta_r^p} = k_M^p. \tag{15}$$

Equation (15) can be integrated after substituting eqns (12) and (13). Thus, the moment–rotation relation based on this model is finally derived as

$$M = (k_M^b - h)\theta_r^p - \delta_{in} \ln [1 + (k_M^b \theta_r^p - M)/\delta_{in}]. \tag{16}$$

The hardening shape parameter h is determined from eqn (16) such that eqn (16) best curve-fits the modified exponential model given by eqn (11). With the above connection model, the tangent stiffness equations for connections are given by

$$\Delta M_i = \Delta K_{Mij} \Delta \alpha_j$$

$$\Delta K_{M11} = \Delta K_{M22} = -\Delta K_{M12} = -\Delta K_{M21} = \Delta k_M \tag{17a,b}$$

where Δk_M is expressed as follows according to the loading states.

Continuous loading or loading up to the first unloading

$$\Delta k_M = \sum_{i=1}^{m} A_i \left\{ \frac{1}{2ic} \exp(-\theta_r/2ic) \right\} + \sum_{j=1}^{n} R_j H(\theta_r - T_j). \tag{18}$$

Unloading, reversed loading or reloading

$$\Delta k_M = k_M^{\xi} k_{MI}/(k_M^{\xi} + k_{MI}). \tag{19}$$

in which k_{MI} is the initial stiffness of the connection and k_M^{ξ} is given by eqn (12).

4. ANALYSIS OF INELASTIC CRITICAL BEHAVIOR

4.1. *General*

Following the usual procedure in the matrix stiffness method, the structural stiffness equation can be derived by assembling the member and connection stiffness equations, respectively, given by eqns (4) and (11) or (16). The structural stiffness equation so derived is nonlinear, and hence critical points may exist, i.e. bifurcation points and limit points, on the equilibrium path. Thus, special attention has to be paid to analyze the behavior around the critical points, since the structural tangent stiffness becomes singular at these points.

In the analysis of the nonlinear equilibrium path, except for the bifurcation points, we employ the arc-length method. As has been confirmed in elastic systems, this method can remove the singularity at the limit points, and the critical behavior around these points can be analyzed with good accuracy. The arc-length method used here is a standard type and no special explanation is made here. Different from the incremental method used primarily for the customary inelastic analysis, the present method further employs the Newton–Raphson iterative procedures in order to obtain convergent solutions. This is because the inelastic $M - \theta_r$ relation is given in terms of the total quantities, as in eqns (11) and (16).

At the bifurcation points for perfect systems, the solution is inherently nonunique, and the singularity of the tangent stiffness matrix cannot be eliminated even by using the arc-length method. Comparing with elastic systems, the bifurcation behavior of semi-rigid frames becomes much more complicated due to the inelastic behavior of connections. Thus, up to the present time, there is no adequate numerical method available which can be used to analyze this inelastic bifurcation of semi-rigid frames accurately.

Herein, we shall present an accurate method which can not only identify the bifurcation point, but also trace the bifurcation path. This method is simple because it only utilizes the tangent stiffness equation along with the Hill's theory of uniqueness and stability for elastic–plastic solids (Hill, 1958). The above method will be explained in some detail in the following.

4.2. *Application of uniqueness criterion to bifurcation analysis*

(a) *Sufficient condition of uniqueness expressed in matrix form.* The bifurcation point is interpreted as a point where the solution of the nonlinear stiffness equation ceases to be unique for a given load condition. The sufficient condition of uniqueness is given by Hill

for elastic–plastic solids. Herein, first, we use the tangent stiffness matrix to express Hill's condition in a form that can be applied to the present matrix analysis. Next, this matrix condition is reduced to a simpler form, taking into account the structural property of semi-rigid frames. Using this simplified form of the sufficient condition for uniqueness, the bifurcation behavior of semi-rigid frames is then investigated theoretically.

For a structural system, it is assumed that the incremental stiffness equations on a fundamental path and on a bifurcation path are respectively expressed as follows at a bifurcation point:

$$\Delta F_i = \Delta K^{\mathrm{f}}_{ij}\Delta u^{\mathrm{f}}_j, \quad \Delta F_i = \Delta K^{\mathrm{b}}_{ij}\Delta u^{\mathrm{b}}_j, \tag{20a,b}$$

where superscripts f and b denote the quantities on the fundamental path and the bifurcation path, respectively, and this notation is used hereinafter.

At the bifurcation point, both eqns (20a) and (20b) hold simultaneously, thus resulting in the following equation:

$$\Delta K^{\mathrm{b}}_{ij}\Delta u^{\mathrm{b}}_j - \Delta K^{\mathrm{f}}_{ij}\Delta u^{\mathrm{f}}_j = 0. \tag{21}$$

Multiplying $(\Delta^{\mathrm{b}}_i - \Delta u^{\mathrm{f}}_i)$ at both sides of eqn (21) yields

$$\Delta\Pi = (\Delta u^{\mathrm{b}}_i - \Delta u^{\mathrm{f}}_i)\Delta K^{\mathrm{f}}_{ij}(\Delta u^{\mathrm{b}}_j - \Delta u^{\mathrm{f}}_j) + (\Delta u^{\mathrm{b}}_i - \Delta u^{\mathrm{f}}_i)(\Delta K^{\mathrm{b}}_{ij} - \Delta K^{\mathrm{f}}_{ij})\Delta u^{\mathrm{b}}_j = 0. \tag{22}$$

Equation (22) is the necessary condition for bifurcation to occur. Conversely, the sufficient condition for the uniqueness of solutions can be expressed as follows, considering the stability condition:

$$\Delta\Pi > 0. \tag{23}$$

This criterion corresponds to Hill's condition expressed in terms of the tangent stiffness matrix. Furthermore, eqn (22) can be rewritten in a more convenient and simpler form, taking into account the structural property of semi-rigid frames. In the present structural model, the inelastic behavior is considered only for connections. Thus, the second term on the right-hand side of eqn (22) is simplified to

$$\Delta\Pi = (\Delta u^{\mathrm{b}}_i - \Delta u^{\mathrm{f}}_i)\Delta K^{\mathrm{f}}_{ij}(\Delta u^{\mathrm{b}}_j - \Delta u^{\mathrm{f}}_j) + \sum_{e=1}^{n_c} (\Delta k^{\mathrm{b}}_{\mathrm{M}e} - \Delta k^{\mathrm{f}}_{\mathrm{M}e})(\Delta\theta^{\mathrm{b}}_{re} - \Delta\theta^{\mathrm{f}}_{re})\Delta\theta^{\mathrm{b}}_{re}, \tag{24}$$

where Δk_{M} is the tangent stiffness of a connection given by eqn (18) or (19), and $\Delta\theta_r$ is the incremental relative rotation of the connection. Subscript e denotes the connection number and n_c is the total number of connections. However, Σ on the right-hand side of eqn (24) implies the summation from 1 to n_c with respect to the quantities with subscript e and the summation convention is not applied within Σ.

Using eqns (22) and (24), the bifurcation behavior of perfect rectangular frames with semi-rigid connections is examined in the following. Loading conditions considered here are of two types, as illustrated in Fig. 4. One is distributed loads, applied vertically on beams, and the other is concentrated loads on columns. Both are increased monotonically up to the bifurcation. These loading conditions are chosen from the consideration of practical importance in customary building frames.

(b) *Bifurcation of rectangular frames under distributed loads applied on beams.* Based on Hill's condition, Hutchinson (1972) generally showed the inelastic bifurcation behavior of elastic–plastic solids for the case when the parts of the solids that have currently yielded, are loading along the fundamental equilibrium path in the direction of increasing external load. Under the increase of the distributed load vertically applied on beams, it is clear that all beam-to-column connnections in the present structures are in a loading state on the

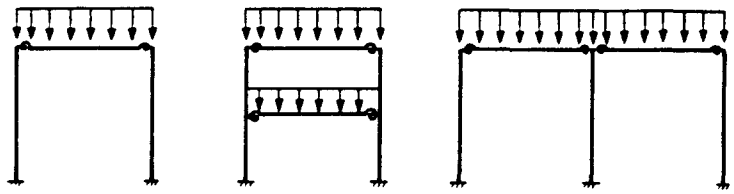

(a) Distributed loads applied on beams

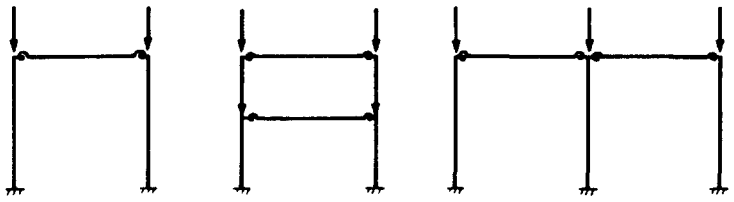

(b) Concentrated loads applied on columns

Fig. 4. Loading conditions of rectangular frames.

fundamental equilibrium path. Thus, the present semi-rigid frames are expected to exhibit the same bifurcation behavior as generally shown by Hutchinson.

Herein, focusing on the connection behavior, we shall examine the specific bifurcation phenomena of semi-rigid frames. Since eqn (22) holds at bifurcation, we can check the buckling phenomena by examining the case in which this equation is satisfied.

Along the fundamental equilibrium path, the connections of the present frames are loading as

$$\Delta\theta_{re}^{f} > 0. \tag{25}$$

Thus, the following condition holds from the constitutive model of connections, according to whether the connections load or unload along the bifurcation path:

$$\Delta k_{Me}^{b} = \Delta k_{Me}^{f} \quad \text{for} \quad \Delta\theta_{re}^{b} \geqslant 0. \tag{26a}$$

$$\Delta k_{Me}^{b} > \Delta k_{Me}^{f} \quad \text{for} \quad \Delta\theta_{re}^{b} \leqslant 0. \tag{26b}$$

Considering eqns (25) and (26), the second term of eqn (24) is positive or zero as

$$\sum_{e=1}^{n} (\Delta k_{Me}^{b} - \Delta k_{Me}^{f})(\Delta\theta_{re}^{b} - \Delta\theta_{re}^{f})\Delta\theta_{re}^{b} \geqslant 0. \tag{27}$$

The equals sign of the above equation is possible when the connections deform along the bifurcation path in such a manner as

$$\Delta\theta_{re}^{b} \geqslant 0. \tag{28}$$

Noting that ΔK_{ij}^{f} is positive definite below the tangent modulus load determined by the condition $|\Delta K_{ij}^{f}| = 0$, the tangent modulus load is the lowest load where eqn (24) becomes zero. This implies that the first possible bifurcation occurs at the tangent modulus load. In this case, $\Delta\theta_{re}^{b}$ satisfies eqn (28) and $(\Delta u_i^{b} - \Delta u_i^{f})$ coincides with the eigenvector of ΔK_{ij}^{f}. This bifurcation behavior of semi-rigid frames agrees exactly with the general notions given by Hutchinson (1972). As the present semi-rigid frames exhibit the sway mode of buckling, some connections load, whilst others unload along the bifurcation path. Thus, in view of

eqn (28), the bifurcation of semi-rigid frames under the present load condition is characterized by the behavior that the increment of the relative rotation is zero in the unloading connections at the instant of bifurcation.

(c) *Bifurcation of rectangular frames under concentrated loads applied on columns.* Under the concentrated loads, it is convenient to classify the bifurcation behavior into two cases, according to whether or not the connections load before bifurcation. In order for the connections not to load before bifurcation, the ratio of the magnitude of concentrated loads applied vertically on columns, has to coincide with that of the cross-sectional areas of the corresponding columns. The connections usually load, except for the frames mentioned above.

When the connections load before bifurcation, the bifurcation behavior of the present structure is basically the same as that shown in Section 4.2(b) for the frames under distributed loads applied on beams. Thus, we need only explain the case when the connections do not load before bifurcation. In this case, both $\Delta k^{f}_{M_i}$ and $\Delta k^{b}_{M_i}$ take the same value, i.e. the initial stiffness of the connections and the second term of eqn (24) becomes zero. Accordingly, eqn (24) becomes zero at the tangent modulus load when $(\Delta u^{b}_{j} - \Delta u^{f}_{j})$ coincides with the eigenvector of ΔK^{f}_{ij}, and bifurcation occurs at this load.

From the coincidence between $\Delta k^{f}_{M_i}$ and $\Delta k^{b}_{M_i}$, the bifurcation phenomena in this case is exactly the same as that of elastic systems. As is well known, the bifurcation point of elastic rectangular frames of concern is symmetric, where the bifurcation occurs without the change of applied loads (Thompson and Hunt, 1973; Britvec, 1973). It should be noted that a *symmetric point of bifurcation* (Thompson and Hunt, 1973) does not necessarily exhibit a symmetric buckling mode of deformation, as can be seen from the sway mode of buckling in the present case. Noting the condition of $\Delta K^{f}_{ij} = \Delta K^{b}_{ij}$ as well as the bifurcation phenomena that the applied loads do not change at the instant of bifurcation, eqn (20b) is reduced to

$$\Delta F_i = \Delta K^{f}_{ij} \Delta u^{b}_{j} = 0. \tag{29}$$

From eqn (29), the incremental displacement Δu^{b}_{j} along the bifurcation path is obtained as the eigenvector of ΔK^{f}_{ij}.

4.3. *Numerical method for bifurcation analysis*

The present numerical method makes use of the information obtained in Section 4.2. The bifurcation analysis consists of two steps, i.e. that of identifying a bifurcation point and of tracing a bifurcation path.

To identify the lowest possible bifurcation load, first we calculate the tangent modulus load. The tangent modulus load corresponds to the singular point where $|\Delta K^{f}_{ij}| = 0$. However, different from the *limit point*, this singularity, which is inherent, cannot be eliminated by the use of the arc-length method. In order to obtain the tangent modulus load accurately, it is necessary to calculate the displacements on the fundamental path up to this load. For this purpose, we have to remove the singularity at the tangent modulus load. Since this singularity results from the existence of the sway mode of deformation, we therefore restrain the frames such that they exhibit only the symmetrical mode of deformation, corresponding to the deformation on the fundamental equilibrium path. An example of this restraint is shown in Fig. 5. With this restraint, the displacements on the fundamental path can be obtained without any difficulty, even at the tangent modulus load. Thus, using the displacements so obtained, we can accurately evaluate the value of $|\Delta K^{f}_{ij}|$. From the condition $|\Delta K^{f}_{ij}| = 0$, the tangent modulus load can be calculated with a required accuracy, using the *bisection method.*

Once the lowest bifurcation point is identified, a bifurcation path is traced from this point.

If the connections load before bifurcation, initial incremental displacements along the bifurcation path are determined by the fact that the increments of relative rotation are zero in the unloading connections, at the instant of bifurcation. In the present numerical analysis,

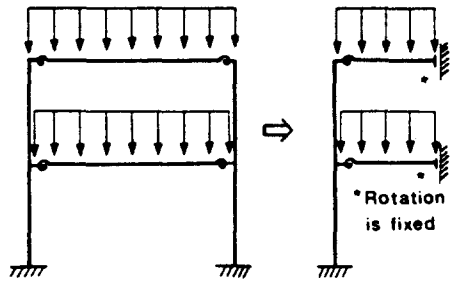

Fig. 5. Restrained model for the analysis of fundamental equilibrium path.

we first assume the locations of the unloading connections to form the structural tangent stiffness matrix ΔK_{ij}^{b}, at the instant of bifurcation. Then, using this tangent stiffness matrix, we calculate Δu_i^{b} under a load increment to evaluate the incremental relative rotations of connections. This is to confirm the validity of the above assumption. If the calculated results coincide exactly with the asumption, Δu_i^{b} so obtained corresponds to the initial incremental displacement along the bifurcation path. If there are some differences between the assumption and the calculated results, the assumption is modified until it agrees with the calculated results. Since connections take either loading or unloading stiffness, all the possibilities which need to be examined are 2^{n_c} where n_c is the total number of connections. In most cases, the number of possibilities is considerably reduced by making use of the information about the possible buckling mode.

On the other hand, when the connections do not load before bifurcation, semi-rigid rectangular frames exhibit a *symmetric point of bifurcation* at the tangent modulus load. Thus, similar to elastic systems, the bifurcation path can be traced using the eigenvector of ΔK_{ij}^{t} as the initial incremental displacement.

Last but not least, if there is little difference between the loading and the unloading stiffness of connections, the value ΔK_{ij}^{b} sometimes becomes numerically singular at the tangent modulus load. As a result, we may experience some numerical difficulty caused by the above method, intended for the analysis of bifurcation with unloading in connections. More specifically, this may happen in the analysis of frames under concentrated loads applied on columns. In this case, owing to the small axial deformation of columns, the relative rotations of connections become small before bifurcation, which results in little difference between the loading and unloading stiffness of connections. This in turn leads to a bifurcation phenomena that is almost the same as that of the frames where connections do not load before bifurcation. Thus, following the elastic bifurcation analysis, the components of the eigenvector ΔK_{ij}^{t} are used as trial incremental displacements to obtain the bifurcation path.

5. NUMERICAL EXAMPLE

5.1. *Test frames*

Three types of rectangular frames with fixed base as shown in Fig. 6, are analyzed to show the validity of the proposed method as well as to examine their critical behavior. These frames are designed on the basis of Type two construction in AISC/ASD (AISC, 1978) under the loads described in Table 1. The design loads along with the height and bay width of the frames under consideration, are exactly the same as those of the two-story single-bay frame shown by Moncarz and Gerstle (1981). They chose the connections from among the top, and seat angles tested by Hechtmann and Johnson (1947); Specimen No. 23 and No. 25 were selected respectively for the upper and lower beams. Herein, due to lack of information about Specimen No. 25 as well as for simplicity, Specimen No. 23 is used for all connections throughout the frames. The moment–rotation curve for this connection under monotonic loading is illustrated in Fig. 2, where the curve expressed by the modified exponential model is also shown for comparison. The constants of the modified

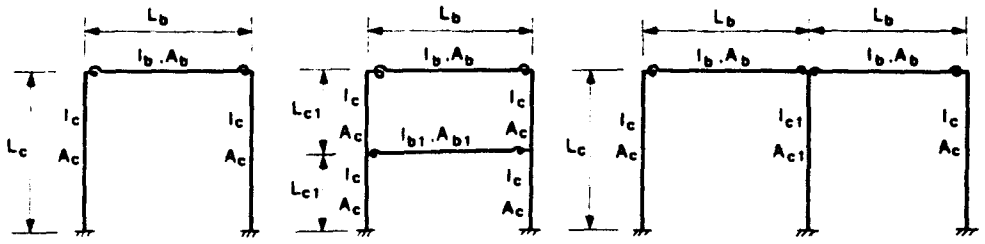

Portal frame	Two-story,one-bay frame	One-story,two-bay frame
I_c =7,076 cm^4 A_c =57.03 cm^2	I_c =7,076 cm^4 A_c =62.65 cm^2 I_{b1}=35.080 cm^4 A_{b1} =83.87 cm^2	I_c =3,430 cm^4 A_c =45.68 cm^2 I_{c1}= 9.906 cm^4 A_{c1} =56.71 cm^2
I_b=15.610 cm^4 A_b =58.84 cm^2 L_b =L_c =2L_{c1} =731.5 cm E_b =E_c =1.998x10^5 MPa		

Fig. 6. Geometry of rectangular frames.

Table 1. Applied loads

Dead load (vertical)	q = 0.335 N cm^{-1} or 0.245 kN cm^{-1} of each girder
Live load (vertical)	p = 0.239 N cm^{-1} on the lower floor of the two-story frame only, or 0.175 kN cm^{-1} of the lower grider
Wind load (horizontal)	w = 0.0957 kN cm^{-1} which results in the concentrated floor loads: W_1 = 25.6 kN for the floors of the one-story frames and the lower floor of the two-story frame, W_2 = 12.8 kN for the upper floor of the two-story frame

Table 2. Constants of modified exponential model

C = 0.17,345,750		
A_i = 0.15,077,925 x 10^1,	−0.74,457,301 x 10^1,	0.13,416,943 x 10^4,
0.68,622,477 x 10^2,	−0.22,747,253 x 10^4,	0.15,788,006 x 10^4
R_j = 0.18,289,890 x 10,	T_j = 9.78	

A_i (i = 1–6), R_j (j = 1): (kN, m), C, T_j (j = 1): (radian).

Table 3. Constants of bounding surface model (kN, m)

Bounding line:	M = 1.829 θ_r^2 + 102.7
Initial stiffness:	k_{MI} = 142.7
Hardening shape parameter:	h = 21.34

exponential model are summarized in Table 2. After a first unloading occurs in the connection, the *bounding surface model* explained previously in Section 3 is used. The hardening shape parameter h, the initial stiffness k_{MI}, and the equation for the bounding line are determined as shown in Table 3, making use of the data for monotonic loading.

5.2. *Frames without load history*

We examine here the critical behavior of frames without the initial imperfection caused by the history of cyclic wind load. To analyze the bifurcation of a perfect system, only the vertical load is applied. As explained previously in Section 4.2, two types of vertical loads

shown in Figs 7(a)–7(c) and Figs 7(a′)–7(c′) are taken into account from the consideration of practical importance in customary building frames. One is the distributed load applied on beams, and the other is the concentrated load on columns. In addition, the concentrated horizontal loads with several magnitudes as indicated in Figs 7(a)–7(c) and Figs 7(a′)–7(c′) are applied at each floor in order to investigate the transition of the critical behavior from the perfect system to the imperfect one. In the imperfect system, a sequential loading is considered, i.e. the horizontal loads are applied first, followed by the vertical loads. Since

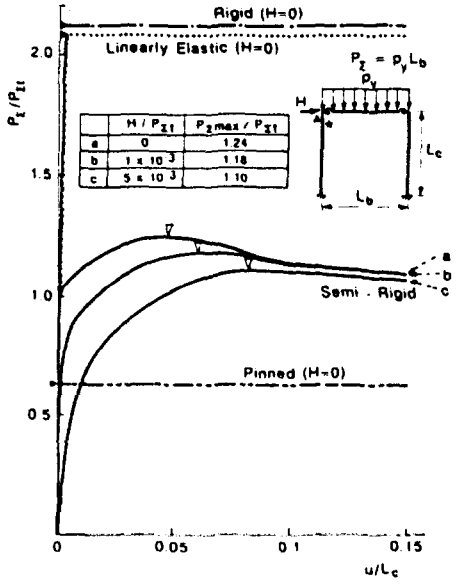

(a) Portal frame under distributed load

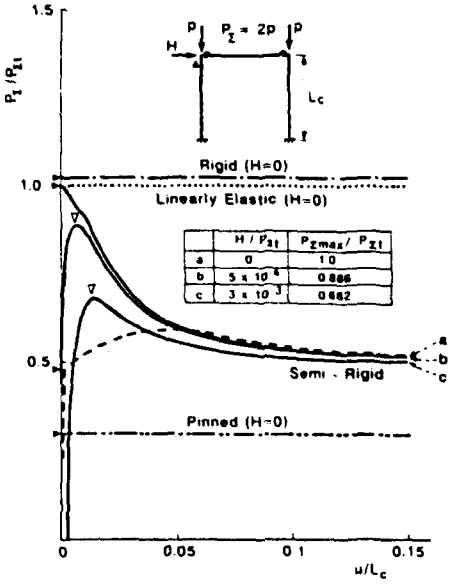

(a′) Portal frame under concentrated load

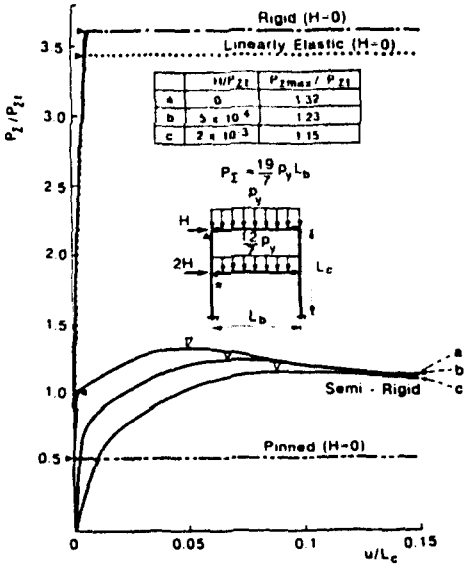

(b) Two-story, two-bay frame under distributed load

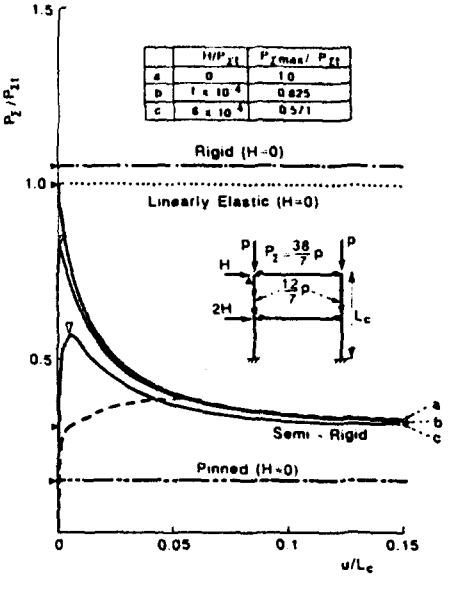

(b′) Two-story, two-bay frame under concentrated load

Fig. 7. Vertical-load vs horizontal-displacement relations for rectangular frames: $P_{\Sigma max}$: maximum load; $P_{\Sigma t}$: tangent modulus load; ▲: node whose horizontal displacement u is shown; ▶: bifurcation point; ▽: limit point; *: connection whose increment of relative rotation becomes zero at the instant of bifurcation; ————: equilibrium path of semi-rigid frame under distributed load.

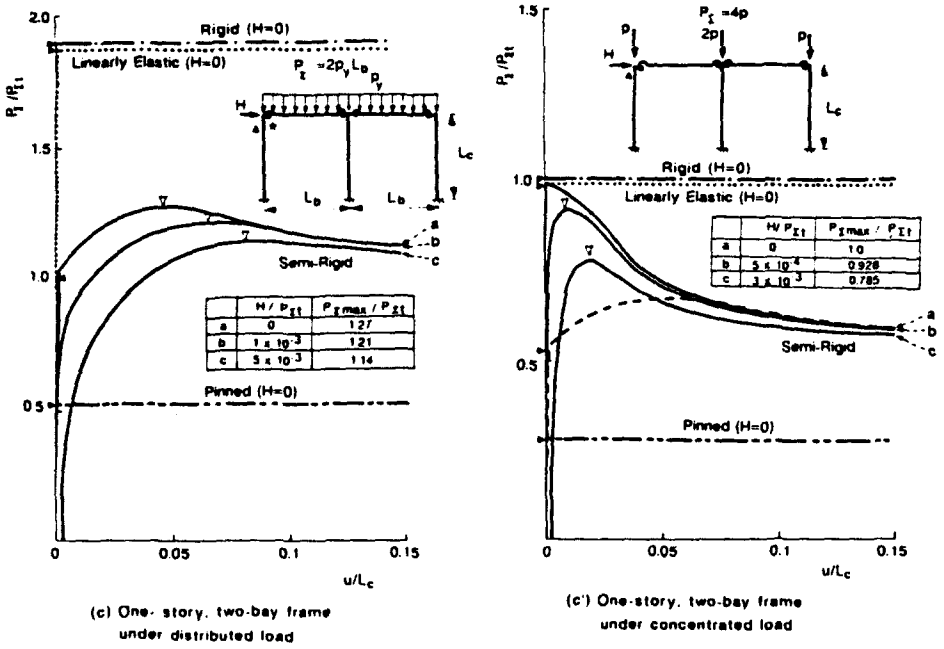

Fig. 7. *Continued.*

the arc-length method is used in the numerical procedure, the arc-length of vertical-load vs displacement curve is increased monotonically in each load sequence.

The results of the numerical analysis are illustrated in Figs 7(a)-7(c) and Figs 7(a')-7(c'), in terms of the vertical-load vs horizontal-displacement relations, classified according to the types of structures as well as the loading conditions. For comparison, these figures also include the post-bifurcation equilibrium curves of frames with pinned or rigid connections, together with those of frames with linearly elastic connections. The elastic constant for these connections is determined such that it coincides with the initial stiffness of the connection curve as shown in Fig. 2. In Figs 7(a')-7(c'), the curves shown by broken lines correspond to perfect systems under vertically distributed loads and these curves are added here to show the difference due to the loading condition.

First, we examine the critical behavior under the distributed loads vertically applied to beams. From Figs 7(a)-7(c), the characteristics of the load-displacement relations are almost the same, regardless of the types of structure. Perfect systems first exhibit bifurcation at the tangent modulus load. However, different from elastic rectangular frames with pinned, rigid or linear elastic connections, the load increases continuously up to the limit point in the post-bifurcation range. This post-bifurcation behavior qualitatively agrees with that predicted from the general theory (Hutchinson, 1972). In all imperfect systems, although a bifurcation does not occur, limit points of the same type can also be found on the equilibrium path. These limit points are located on a load level higher than the tangent modulus load. As theoretically explained in Section 4.2, the increment of the relative rotation becomes zero in the unloading connections, when the bifurcation occurs at the tangent modulus load. This fact is confirmed in the present analysis. The connections whose incremental relative rotation becomes zero are marked with * in Figs 7(a)-7(c).

Next, we shall investigate the behavior of frames under the concentrated load vertically applied on columns. As can be seen from Figs 7(a')-7(c'), the characteristics of these load-displacement curves are rather different from either those cases under distributed loads or those with pinned rigid or linearly elastic connections. That is, in the present case, the loads applied to perfect systems drop dramatically after the bifurcation occurs at the tangent modulus load. As for the imperfect systems, although the limit-load instability occurs as in the previous case under distributed loads, all the maximum loads are smaller than the corresponding tangent modulus loads. These maximum loads are lowered by the increase

of lateral loads given as an initial imperfection. As the lateral displacements increase, all load–displacement curves gradually approach the tangent modulus load of the frames under distributed loads.

To summarize the above results, the critical behavior of semi-rigid frames is much influenced by the vertical load conditions. This is quite different from the behavior of customary frames with rigid or pinned joints. In the following, we shall explain why the critical behavior of semi-rigid frames is so much influenced by the loading conditions. Since this influence is most evident in a perfect system, a perfect system is used here for explanation.

If the distributed loads are applied on beams, the connections are loaded. This loading continuously reduces the tangent stiffness of these connections up to the bifurcation point. However, once the bifurcation occurs, some of the connections unload and their stiffness increases and consequently, the vertical loads increase even after bifurcation. On the other hand, when the concentrated loads are applied to columns, connections are not loaded before bifurcation, thus resulting in no reduction in stiffness. Therefore, these bifurcation loads coincide with those of the frames with linearly elastic connections, whose elastic constant corresponds to the initial stiffness of the connection curve. However, when bifurcation occurs, the connections suddenly deform. Due to the nonlinear property of the connection curve in Fig. 2, this deformation reduces the connection stiffness, thus resulting in instability just after the bifurcation.

5.3. *Frames with history of cyclic wind load*

Since the beam-to-column connections exhibit inelastic behavior, the critical behavior of frames with a history of cyclic wind load is expected to behave differently from that without it.

Herein, prior to the application of cyclic wind load, the vertical load, either distributed or concentrated, is increased to its design level as shown in Table 1. Since the design load is not given for concentrated loads vertically applied on columns, this load is determined in such a way that the total value of the concentrated load coincides with that of the distributed design load. The history of cyclic wind load is given in the following manner. First, the horizontal wind load is increased monotonically up to the maximum value and then reduced to zero. Next, the wind direction is reversed and this load is applied from the opposite side in a similar manner. This wind cycle is repeated until the hysteresis loops of connections become convergent. In the present wind cycles, two amplitudes are considered. One corresponds to the design wind load in Table 1 and the other is twice this value. Figures 8(a) and 8(a′) show how these hysteresis loops of semi-rigid connections become convergent under the present cyclic wind loads. Herein, for simplicity, we only show the results for portal frames under cyclic wind loads with a larger amplitude. From Figs 8(a) and 8(a′), it can be seen that the convergence of hysteresis loops differs according to whether the vertical load is applied to columns or to beams. That is, the hysteresis loops for the latter case converge slower than those for the former. This tendency is also observed in other frames.

To examine the critical behavior, the vertical load is increased from the design load level after the removal of the wind load. Similar to the analysis of frames without load history, the arc-length of the vertical load-displacement curve is increased monotonically. The vertical-load vs horizontal-displacement relations obtained from the present analysis are illustrated in Figs 9(a)-9(c) and Figs 9(a′)-9(c′), classified in a similar manner to that of Figs 7(a)-7(c) and Figs 7(a′)-7(c′). For comparison, the results for the perfect system without load history are also shown in these figures.

As can be seen from these figures, the load history caused by the wind load has a significant influence on the critical behavior of frames with concentrated loads, applied vertically to columns. Due to the initial imperfection resulting from a load history, these frames only exhibit the *limit load instability* similar to the imperfect system in Figs 7(a′)–7(c′). This limit load is located at the load level lower than the bifurcation point of a perfect system. This tendency becomes more pronounced as the amplitude of the cyclic wind

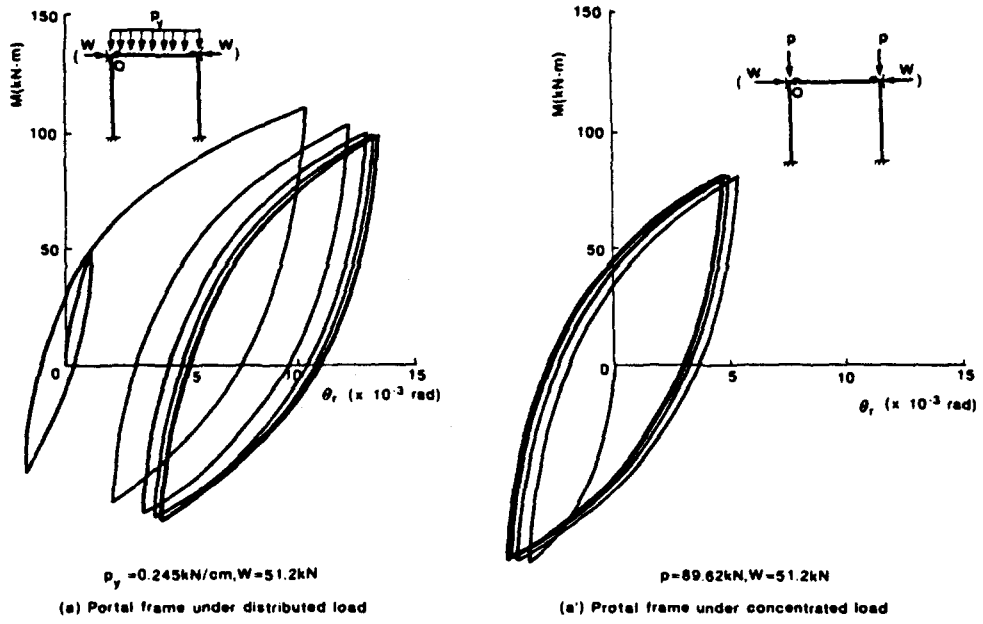

Fig. 8. Hysteresis loops of connections under cyclic wind load: ○: connection whose hysteresis loop is shown.

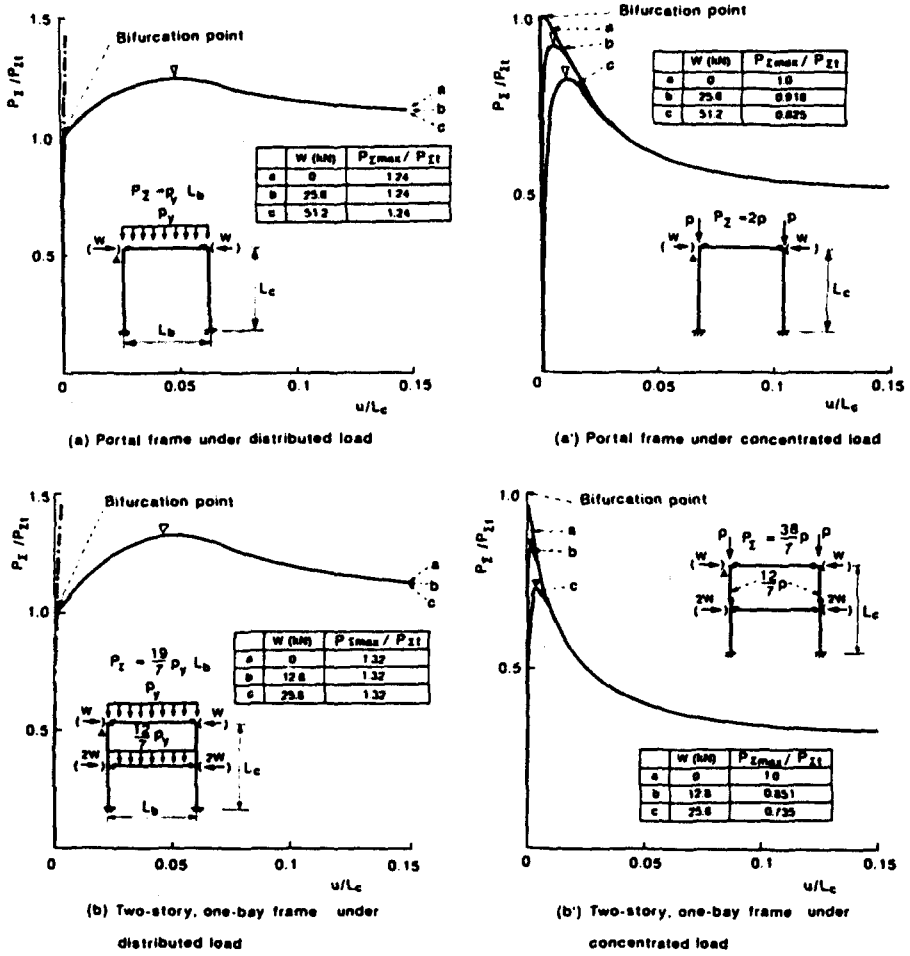

Fig. 9. Vertical-load vs horizontal-displacement relations for rectangular frames with history of cyclic wind load: W: magnitude of cyclic wind load; $P_{\Sigma max}$: maximum load; $P_{\Sigma t}$: tangent modulus load; ▲: node whose horizontal displacement is shown; ▽: limit point; —·—·—: fundamental equilibrium path.

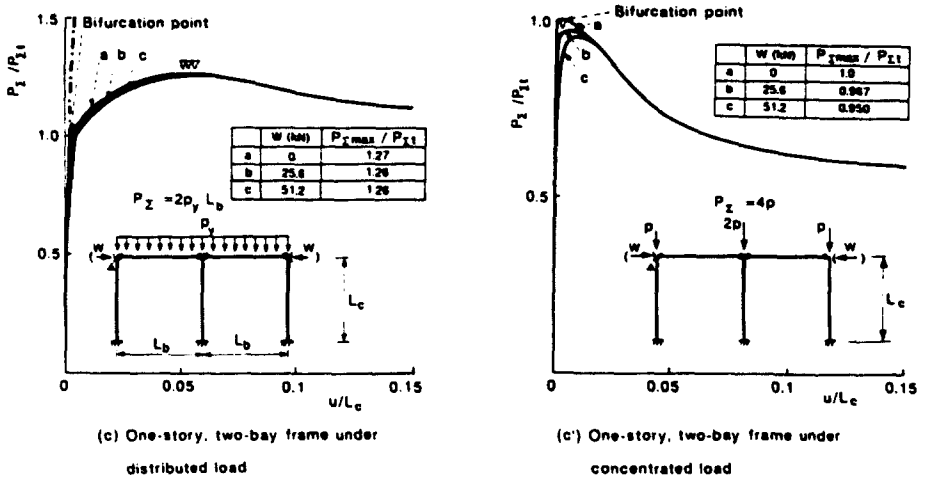

(c) One-story, two-bay frame under distributed load

(c') One-story, two-bay frame under concentrated load

Fig. 9. *Continued.*

load becomes large. However, with the increase in horizontal displacements, the load–displacement curves rapidly approach those of perfect systems.

In contrast to the above case, most of the load–displacement curves of frames under distributed load are the same, regardless of whether the frames have load history or not. One exception is the example of one-story, two-bay frame. In this case, the bifurcation does not occur due to the imperfection caused by the load history. However, even for this case, its load–displacement curve almost coincides with that of a perfect system. The critical behavior of the other frames is not influenced by their load history. That is, in spite of a load history, the portal frame as well as the two-story, one-bay frame exhibit both bifurcation and limit load instability, coincident exactly with that of the corresponding perfect systems with virgin connections. In the above cases, the imperfection caused by the cyclic wind load is gradually reduced with an increase in the distributed load applied on beams, and almost completely disappears before bifurcation occurs. This can be explained further in the following.

From the constitutive relation in Fig. 2, the tangent stiffness of connections decreases with an increase in applied moment. This implies that the increment of moment is more rapid in connections with less deformation. In other words, a connection with less deformation, deforms with a higher rate than that with a larger deformation. As a result, with an increase of the loads applied to beams, the deformations of frames are adjusted naturally such that they become symmetric, thus resulting in a perfect system.

6. CONCLUDING REMARKS

In this paper, we have presented an accurate, yet simple method that can be used to analyze the inelastic critical behavior of semi-rigid frames, with special emphasis on bifurcation and limit-load instability.

Using the proposed method, the critical behavior of several rectangular frames with semi-rigid connections is accurately analyzed. In the present analysis, we have also investigated the effects of imperfections due to a history of cylic wind load on the critical behavior.

We have found that the buckling of semi-rigid frames is greatly influenced by the vertical load conditions. This is quite different from the customary frames with pinned, rigid or linearly elastic connections.

If the concentrated loads are applied vertically on columns, the loads of a perfect system drop dramatically after bifurcation and the frame loses its stability. Furthermore, the frame under this load condition is very sensitive to its imperfections, i.e. the imperfection due to horizontal loads and the imperfection resulting from a history of cyclic wind loads. These imperfections considerably reduce the maximum value of vertical loads.

In contrast to the above case, if distributed loads are vertically applied on beams, the loads of a perfect system increase even after bifurcation, and the frame does not lose its stability until the loads reach their limit point. In addition, the frame is less influenced by its imperfections. Specifically, the imperfection caused by a history of cyclic wind loads almost completely disappears in a semi-rigid frame before bifurcation occurs, and its critical behavior virtually coincides with that of a perfect system with virgin connections.

REFERENCES

Ackroyd, M. H. (1979). *Nonlinear inelastic stability of flexibly-connected plane steel frames*. Ph.D. Thesis, Department of Civil Engineering, University of Colorado, Boulder.

AISC (1978). *Specification for the Design, Fabrication of Structural Steel for Buildings*. Chicago, IL.

Chen, W. F. and Kishi, N. (1989). Semi-rigid steel beam-to-column connections: data base and modeling. *J. Struct. Engng, ASCE* **115**(1), 105–119.

Chen, W. F. and Lui, E. M. (1985). Column with end restraint and bending in load and resistance factor design. *Engineering Journal, AISC*, Third Quarter, pp. 105–132.

Cook, N. E. (1983). *Strength of flexibly-connected steel frames under load histories*. Ph.D. Thesis, Department of Civil Engineering, University of Colorado, Boulder.

Dafalias, Y. F. and Popov, E. P. (1976). Plastic internal variables formalism of cyclic plasticity. *J. Appl. Mech.* **43**, 645–651.

Goto, Y. and Chen, W. F. (1987a). Second-order elastic analysis for frame design. *J. Struct. Div., ASCE* **113**(7), 1501–1519.

Goto, Y. and Chen, W. F. (1987b). On the computer-based design analysis for the flexibly jointed frames. *J. Construct. Steel Res.* **8**, 203–231.

Goto, Y., Suzuki, S. and Chen, W. F. (1989a). Bifurcation and limit-load instability of flexibly jointed frames. *Proc. International Colloquium on Bolted and Special Structural Joints*, Moscow, May, pp. 80–89.

Goto, Y., Suzuki, S. and Chen, W. F. (1991). Bowing effect on the elastic stability of frames under primary bending moment. *J. Struct. Engng, ASCE* **117**(1).

Goto, Y., Suzuki, S. and Matsuura, S. (1989b). Analysis of critical behavior of flexibly jointed frames. *Proc. JSCE* (in Japanese). October, **410** (I-12), pp. 287–296.

Hechtmann, R. A. and Johnson, B. G. (1947). Riveted semi-rigid beam-to-column building connections. Progress Report No. 1, AISC Publication (Appendix B).

Hill, R. (1958). A general theory of uniqueness and stability in elastic plastic solids. *J. Mech. Phys. Solids* **6**, 236–249.

Hutchinson, J. W. (1972). Post bifurcation behavior in the plastic range. *J. Mech. Phys. Solids* **21**, 163–190.

Jones, S. W., Kirby, P. A. and Nethercot, D. A. (1983). The analysis of frames with semi-rigid connections. A State-of-the-Art Report. *J. Construct. Steel Res.* **3**(2), 1–13.

Lui, E. M. and Chen, W. F. (1986). Analysis and behavior of flexibly-jointed frames. *Engng Struct.* **8**, 107–118.

Mazzolani, F. M. (1987). Influence of semi-rigid connections on the overall stability of steel frames, connection in steel structures. *Proc. Workshop on Connections and the Behavior, Strength and Design of Steel Structures*, Cachan, France, pp. 272–275.

Moncarz, P. D. and Gerstle, K. H. (1981). Steel frames with nonlinear connections. *J. Struct. Div., ASCE* **107**(8), 1427–1441.

Poggi, C. and Zandonini, R. (1987). A finite element for the analysis of semi-rigid frames, connections in steel structures. *Proc. Workshop on Connections and the Behavior, Strength and Design of Steel Structures*, Cachan, France, pp. 238–247.

Riks E. (1979). An incremental approach to the solution of snapping and buckling problems. *Int. J. Solids Structures* **15**, 529–551.

Romstad, K. M. and Subramanian, C. V. (1970). Analysis of frames with partial connection rigidity. *J. Struct. Div., ASCE* **96**(11), 2283–2300.

Simitses, G. J. and Vlahinos, A. S. (1984). Elastic stability of rigidly and semi-rigidly connected unbraced frames. In *Steel Framed Structures* (edited by R. Narayanan), pp. 115–152. Elsevier, London.

Thompson, J. M. T. and Hunt, G. W. (1973). *A General Theory of Elastic Stability*. John Wiley, London.

Yu, C. H. and Shanmugam, N. E. (1986). Stability of frames with semi-rigid joint. *Comput. Struct.* **23**(5), 639–648.